

# Density matrix renormalization group approach for many-body open quantum systems

J. Rotureau<sup>1,2,3</sup>, N. Michel<sup>1,2,3</sup>, W. Nazarewicz<sup>1,2,4</sup>, M. Płoszajczak<sup>5</sup>, and J. Dukelsky<sup>6</sup>

<sup>1</sup> *Department of Physics and Astronomy, University of Tennessee, Knoxville, Tennessee 37996*

<sup>2</sup> *Physics Division, Oak Ridge National Laboratory, Oak Ridge, Tennessee 37831*

<sup>3</sup> *Joint Institute for Heavy Ion Research, Oak Ridge National Laboratory, P.O. Box 2008, Oak Ridge, Tennessee 37831*

<sup>4</sup> *Institute of Theoretical Physics, University of Warsaw, ul. Hoża 69, 00-681 Warsaw, Poland*

<sup>5</sup> *Grand Accélérateur National d'Ions Lourds (GANIL),*

*CEA/DSM - CNRS/IN2P3, BP 55027, F-14076 Caen Cedex, France*

<sup>6</sup> *Instituto de Estructura de la Materia, CSIC, Serrano 123, 28006 Madrid, Spain*

(Dated: October 29, 2018)

The density matrix renormalization group (DMRG) approach is extended to complex-symmetric density matrices characteristic of many-body open quantum systems. Within the continuum shell model, we investigate the interplay between many-body configuration interaction and coupling to open channels. It is shown that the DMRG technique applied to broad resonances in the unbound neutron-rich nucleus <sup>7</sup>He provides a highly accurate treatment of the coupling to the non-resonant scattering continuum.

PACS numbers: 02.70.-c,02.60.Dc,05.10.Cc,21.60.Cs,25.70.Ef

The DMRG method was introduced to overcome the limitations of Wilson-type renormalization group to describe strongly correlated 1D lattice systems with short range interactions [1] (see recent reviews [2, 3]). Extensions of DMRG to 2D lattice models are in general less accurate and require a reduction to a 1D problem by selecting a path in the 2D plane. More recently, by reformulating the DMRG in a single-particle (s.p.) basis, several applications to finite Fermi systems like molecules [4], superconducting grains [5], quantum dots [6], and atomic nuclei [7] have been reported. The main advantage of DMRG is that it can accurately treat configuration spaces of dimensions well beyond the limits of a large-scale diagonalization. The early application of DMRG in the context of the nuclear shell model (SM) in the  $M$ -scheme exhibits some convergence problems that are not yet understood [8]. The first DMRG+SM applications in the angular-momentum-conserving  $J$ -scheme were successfully carried out in Ref. [9] and also recently in Ref. [10]. A similar formalism, known as non-Abelian DMRG, has been previously applied to quantum lattice models [11]. While most of the DMRG studies were focused on equilibrium properties in strongly correlated closed quantum systems with hermitian density matrix, non-equilibrium systems involving non-hermitian and non-symmetric density matrices can also be treated with a DMRG procedure [12]. In this work, we shall present the first detailed test of the DMRG approach to many-body open quantum systems (OQS) described by the Gamow Shell Model (GSM) [13, 14], i.e., the continuum SM in the complex  $k$ -plane. The DMRG approach within the GSM is characterized by complex-symmetric reduced density matrices. We are particularly interested in developing an efficient strategy for selecting most important configurations involving s.p. resonances and non-resonant scattering states that describe many-body unbound states. Our approach was briefly sketched

in Ref. [9].

GSM is the multi-configurational SM with a s.p. basis given by the Berggren ensemble [15] consisting of Gamow (resonant or Siegert) states and the non-resonant continuum of scattering states. The resonant states are the generalized eigenstates of the time-independent Schrödinger equation, which are regular at the origin and satisfy purely outgoing boundary conditions. GSM provides a quasi-stationary formalism for describing the time-dependent processes such as the multi-particle decays. The s.p. Berggren basis is generated by a finite-depth potential, and the many-body states can be expanded in Slater determinants spanned by resonant and non-resonant s.p. basis states [13, 14]. The GSM, which has been up to now applied to weakly bound/unbound atomic nuclei, can be equally applied for the description of other OQS, e.g., open microwave resonators and self-bound atomic systems, such as <sup>3</sup>He<sub>N</sub> neutral droplets at the limits of their stability [16]. Another possible application of the GSM are quantum dots, where the interplay between electron-electron correlations and the continuum coupling yields the transition in the conductance properties.

At present, the principal limitation of GSM applications is the explosive growth in the number of configurations (i.e., dimension of the many-body Fock space) with both the number of active particles and the size of the s.p. space. To ensure completeness of the Berggren basis, for each resonant s.p. state of quantum numbers  $l_j$ , with  $l$  being the orbital angular momentum and  $j$  the total angular momentum, one should include a large set of discrete non-resonant continuum states  $\{(l_j)^{(i)}; i = 1, \dots, M\}_c$  lying on a continuous contour  $L_+^{l_j}$  in the complex  $k$ -plane [13, 14]. These continuum states become new active shells in the many-body framework of GSM and, because of their presence, the dimension of the GSM Hamiltonian matrix grows extremely fast. This ex-

pllosion of the Hilbert space is much more severe than in the standard SM, which deals solely with a limited number of discrete s.p. states. The use of the Berggren ensemble implies a *complex-symmetric* Hamiltonian matrix for the *hermitian* Hamilton operator. Due to the large number of non-resonant continuum shells whose properties vary smoothly along the contour, the GSM Hamiltonian matrix is significantly denser than that of a conventional SM. As a result, matrix operations are more time-consuming in GSM than in SM, and the Lanczos procedure for GSM eigenvectors [13] becomes very slow.

Most of the configurations involving many particles in the non-resonant continuum contribute very little to low-energy GSM eigenfunctions calling for a smart selection of the most important configurations. For that purpose, we propose a new algorithm based on the DMRG procedure for finding the GSM eigenvalues. The main idea is to gradually consider different s.p. shells of the discretized non-resonant continuum in the configuration space and retain only  $N_{\text{opt}}$  optimal states dictated by the eigenvalues of the density matrix with largest modulus. The procedure will be illustrated using the example of many-body resonances in the neutron-unbound nucleus  ${}^7\text{He}$  described in terms of  $N_v=3$  active (valence) neutrons outside the closed core of  ${}^4\text{He}$ .

The s.p. basis is generated by a Woods-Saxon (WS) potential with the radius  $R_0=2$  fm, the depth of the central potential  $V_0=47$  MeV, the diffuseness  $d=0.65$  fm, and the spin-orbit strength  $V_{\text{so}}=7.5$  MeV [13]. This s.p. potential reproduces experimental energies and widths of the s.p. resonances  $3/2_1^-$  (g.s.) and  $1/2_1^-$  (first excited state) in  ${}^5\text{He}$  at  $E=0.745-i0.32$  MeV and  $E=2.13-i2.94$  MeV, respectively. The neutron valence space consists of the  $0p_{1/2}$  and  $0p_{3/2}$  resonant states and the corresponding non-resonant states  $\{p_{1/2}\}_c$ ,  $\{p_{3/2}\}_c$ . The  $L_+^{p_{1/2}}$  contour in the complex- $k$  plane (in the following,  $k$  is expressed in units of  $\text{fm}^{-1}$ ) is defined by a triangle with vertices at  $(\mathcal{R}e(k), \mathcal{I}m(k)) = (0,0)$ ,  $(0.33, -0.33)$ ,  $(0.5,0.0)$ , and a segment along the  $\mathcal{R}e(k)$ -axis from  $(0.5,0)$  to  $(1.0,0.0)$ . Similarly,  $L_+^{p_{3/2}}$  is given by a triangle:  $(0,0)$ ,  $(0.17, -0.17)$ ,  $(0.5,0)$ , and a straight segment from  $(0.5,0)$  to  $(1.0,0)$ . Each segment of these contours is discretized with the same number of points corresponding to the abscissas for Gauss-Legendre quadrature. The GSM Hamiltonian is a sum of the WS potential, representing the effect of an inert  ${}^4\text{He}$  core, and the two-body interaction among valence neutrons. The latter is approximated by a finite-range surface Gaussian interaction [17] with the range  $\mu=1$  fm and the coupling constants depending on the total angular momentum  $J$  of the neutron pair:  $V_0^{(J=0)} = -542$  MeV  $\text{fm}^3$ ,  $V_0^{(J=2)} = -479$  MeV  $\text{fm}^3$ . These constants are fitted to reproduce the binding energies of  ${}^6\text{He}$  and  ${}^7\text{He}$  with respect to the core.

For the purpose of DMRG, the configuration space is divided into two Fock subspaces:  $A$  (built from the

s.p. resonant shells  $0p_{1/2}$ ,  $0p_{3/2}$ ), and  $B$  (built from s.p. non-resonant shells  $\{p_{1/2}\}_c$  and  $\{p_{3/2}\}_c$ ). In the warm-up phase, one calculates and stores all possible matrix elements of suboperators of the Hamiltonian in  $A$ :  $a^\dagger$ ,  $(a^\dagger \tilde{a})^K$ ,  $(a^\dagger a^\dagger)^K$ ,  $((a^\dagger a^\dagger)^K \tilde{a})^L$ ,  $((a^\dagger a^\dagger)^K (\tilde{a}\tilde{a})^K)$ , and constructs all the states  $|k\rangle_A$  with  $n = 0, 1, \dots, N_v$  particles coupled to all possible  $j$ -values. Then, from the sets:  $\{p_{1/2}\}_c$ ,  $\{p_{1/2}\}_c$ , one picks up the first pair of s.p. states, calculates the full set of matrix elements of suboperators for this added pair, and constructs all the states  $|i\rangle_B$  with  $n$  particles ( $n = 0, 1, \dots, N_v$ ). The subspace  $B$  is gradually enlarged by successively adding pairs of non-resonant shells ( $p_{1/2}, p_{3/2}$ ) until the number of states  $|i\rangle_B$  exceeds  $N_{\text{opt}}$ . Then the Hamiltonian is diagonalized in the space  $\{|k\rangle_A |i\rangle_B\}^J$  made of vectors in  $A$  and  $B$ . Obviously, the total number of particles in such states must be kept equal to the total number of valence particles, and the angular momentum  $J$  is conserved. To find the many-body resonance from all the eigenstates,  $|\Psi^J\rangle = \sum c_{ki} \{|k\rangle_A |i\rangle_B\}^J$ , one selects the eigenstate having the largest overlap with the GSM eigenstate in a pole approximation (i.e., diagonalized in the subspace  $A$  only). From this eigenstate, one calculates the reduced density matrix  $\rho_{ii'}^{B,j} = \sum_k c_{ki} c_{ki'}$  with a fixed value of  $j$  in states  $|i\rangle_B$ ,  $|i'\rangle_B$  [11]. By construction, the density matrix  $\rho^B$  is then block-diagonal in  $j$ . Within the metric defining the Berggren ensemble, the density matrix is complex symmetric; hence, its eigenvalues are complex. The reduced density matrix is diagonalized, and  $N_{\text{opt}}$  eigenstates  $|u_\nu\rangle$  having the eigenvalues with the largest absolute values are retained. Those eigenvalues correspond to the most important states in the enlarged set. All the matrix elements of suboperators for the optimized states are recalculated. Then, the next pair of non-resonant continuum shells is added and, again, only  $N_{\text{opt}}$  eigenvalues of the density matrix are kept. This procedure is repeated until the last shell in  $B$  is reached, providing a first guess for the wave function of the system in the whole ensemble of shells forming the basis. From now on, all the s.p. states are considered.

At this point, the warm-up phase ends and the so-called sweeping phase begins. Here, one constructs states with  $0, 1, 2, \dots, N_v$  particles and then the process continues in the reverse direction until the number of vectors becomes larger than  $N_{\text{opt}}$ . If the  $m^{\text{th}}$  pair of  $p$ -shells in  $B$  is reached, the Hamiltonian is diagonalized in the set of vectors:  $\{|k, i_{\text{prev}}\rangle |i\rangle\}^J$ , where  $i_{\text{prev}}$  is a previously optimized state (constructed from first  $m-1$  pairs of shells in  $B$ ), and  $i$  is a new state. The density matrix is then diagonalized and the  $N_{\text{opt}}$   $i$ -states are kept. The procedure continues by adding the  $(m-1)^{\text{st}}$  pair of shells, etc., until the first pair of  $p$ -shells in  $B$  is reached. Then the procedure is reversed again: the first pair of shells is added, then the second, the third, etc.

In the examples presented in this work, the number of s.p. shells included in  $A$  and  $B$  are  $N_r=2$  and  $N_c = 60$

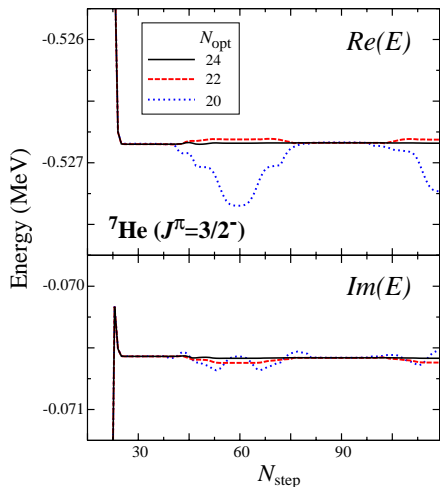


FIG. 1: GSM+DMRG results for the real (top) and imaginary (bottom) parts of the g.s. ( $J^\pi = 3/2^-$ ) energy of  ${}^7\text{He}$  plotted as a function of the number of DMRG steps. The number of states kept during the sweeping phase is  $N_{\text{opt}}=20$  (dotted line), 22 (dashed line), and 24 (solid line).

(30 shells in each continuum:  $\{p_{1/2}\}_c$ ,  $\{p_{3/2}\}_c$ ), respectively. In the warm-up phase, 8 vectors are kept. Figure 1 shows the convergence properties of the ground state (g.s.)  $J^\pi = 3/2^-$  resonance energy in  ${}^7\text{He}$  plotted as a function of the number of DMRG steps  $N_{\text{step}}$ . (As discussed earlier, one step corresponds to adding a pair of  $\{p_{1/2}\}_c$ ,  $\{p_{3/2}\}_c$  shells.) Converged results, manifested by a local plateau at the complex energy  $E=E_0$ , are found after  $N_{\text{step}} \leq 30$  steps. Then, with increasing  $N_{\text{step}}$ , one enters the unstable region ( $40 \leq N \leq 70$ ). A second plateau, corresponding to practically the same energy  $E_0$  as the first plateau (and fairly independent of  $N_{\text{opt}}$ ), appears at  $N_{\text{step}} \sim 90$ . The “plateau-unstable” sequence repeats periodically. It is worth noting that the deviation from  $\mathcal{R}e(E_0)$  can be both positive and negative. This is because the Hamiltonian matrix is not hermitian but complex-symmetric; hence, the usual reasoning based on the Ritz variational principle does not apply.

The behavior of the DMRG procedure, as can be seen in Fig. 1 and Table I, shows a gradual reduction of the energy variation around the plateau with increasing number of sweeps  $N_{\text{sw}}$ . Most importantly, it decreases quickly with the number of states  $N_{\text{opt}}$  kept in the sweeping phase. The relative precision of the DMRG procedure is extremely high:  $\sim 10^{-6}$  for  $N_{\text{opt}}=24$  and  $N_{\text{sw}}=4$ .

Figure 2 illustrates the convergence of the DMRG procedure for the first excited state in  ${}^7\text{He}$ , which is calculated to be a broad resonance with  $\Gamma=3.37$  MeV. Here, 7 vectors are kept in the warm-up phase. The full convergence is attained in about 2 sweeps, i.e., somewhat slower than for the narrow g.s. resonance ( $\Gamma=0.14$  MeV). Still,

$N_{\text{opt}}$	$\Delta E/E$ ( $N_{\text{sw}} = 2$ )	$\Delta E/E$ ( $N_{\text{sw}} = 4$ )
20	$9.4 \times 10^{-4}$	$7.5 \times 10^{-4}$
22	$8.0 \times 10^{-5}$	$4.9 \times 10^{-5}$
24	$3.0 \times 10^{-5}$	$4.7 \times 10^{-6}$
26	$2.1 \times 10^{-5}$	$2.6 \times 10^{-6}$

TABLE I: Relative precision of the real part of the g.s. energy in  ${}^7\text{He}$  as a function of the number of states  $N_{\text{opt}}$  kept in the sweeping phase at the second ( $N_{\text{sw}}=2$ ) and fourth ( $N_{\text{sw}}=4$ ) sweep of GSM+DMRG.

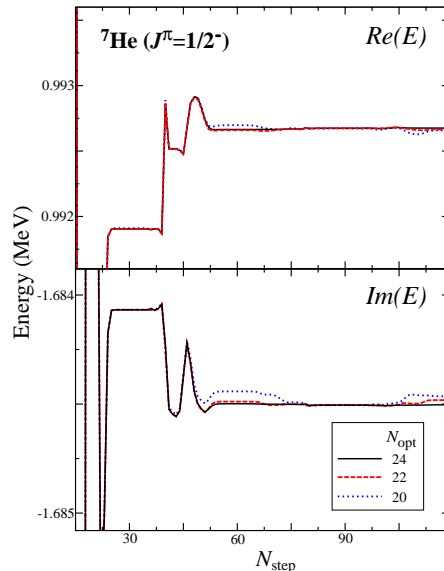


FIG. 2: Similar to Fig. 1 except for the first excited state ( $J^\pi = 1/2^-$ ) in  ${}^7\text{He}$ .

the resulting plateau is excellent. Again, as in Fig. 1,  $E_0$  is practically independent of  $N_{\text{opt}}$ . These two examples demonstrate that the proposed DMRG algorithm is extremely efficient in selecting the most important non-resonant continuum structures.

A major problem in studies of OQS is to maintain the completeness of the many-body basis containing contributions from *discretized* non-resonant s.p. continua. In this respect, the Berggren ensemble is not different: it has to be discretized for any practical applications of the GSM. The accuracy of discretized many-body calculations relies upon the independence of calculated observables such as energies, transition probabilities, and cross sections from the number of s.p. shells in the complex non-resonant continuum. To illustrate this point, we show in Fig. 3 the g.s. energy of  ${}^7\text{He}$  as a function of the total number of s.p. shells  $N_{\text{sh}}$ . One can see that the dependence of  $\mathcal{R}e(E)$  and  $\mathcal{I}m(E)$  on  $N_{\text{sh}}$  is not monotonic, showing oscillations which disappear only if a sufficiently

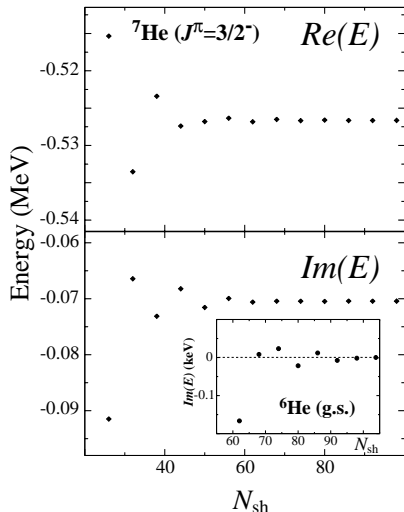


FIG. 3: Convergence of the real (top) and imaginary (bottom) parts of the g.s. energy of  ${}^7\text{He}$  as a function of the total number of shells  $N_{\text{sh}} (\equiv N_c + N_r = N_c + 2)$  included in the s.p. basis. As in Fig. 1, 8 vectors are kept in the warm-up phase. In the sweeping phase,  $N_{\text{opt}}=22$  states are kept. The inset shows the imaginary part of the g.s. energy of  ${}^6\text{He}$  as a function of  $N_{\text{sh}}$ . Here,  $N_{\text{opt}}=4$  (10) vectors were kept in the warm-up (sweeping) phase.

dense discretization is applied. A similar oscillatory pattern is seen in the imaginary part of the g.s. energy of  ${}^6\text{He}$  (shown in the inset). Since  ${}^6\text{He}$  is bound, the deviation of  $\text{Im}(E)$  from zero is due to too coarse discretization; the completeness is practically achieved for  $N_{\text{sh}}=70$ . While the error due to an insufficient number of non-resonant shells is of the order of  $10^{-2}$  keV, the accuracy of DMRG is in the range of  $10^{-6}$  keV.

The results shown in Figs. 1-3 demonstrate that the fully converged GSM results with respect to both the number of sweeps and the number of shells in the discretized continua can be obtained using the GSM+DMRG algorithm. The rank of the biggest matrix to be diagonalized in GSM+DMRG grows extremely slowly with  $N_{\text{sh}}$ . In the example shown in Fig. 3, it changes from  $d=941$  to  $d=1001$ , whereas the dimension of the GSM matrix in the  $J$ -coupling scheme varies as  $D \propto N_{\text{sh}}^3$ , from  $D=6149$  for  $N_{\text{sh}}=26$ , to  $D=332,171$  for  $N_{\text{sh}}=98$ . Hence, the gain factor  $D(N_c)/d(N_c) \sim N_{\text{sh}}^3$  quickly grows with increasing  $N_c$  (or the size of block  $B$ ).

Our results indicate that (i) the complex energy  $E_0$  at the DMRG plateau very weakly depends on  $N_{\text{opt}}$ , and (ii) the precision of calculated complex energies weakly depends on  $N_{\text{sh}}$ , provided that  $N_{\text{sh}}$  is sufficiently large. This means that the convergence features of the GSM+DMRG procedure can be tested by varying  $N_{\text{sh}}$

and  $N_{\text{opt}}$ . Once those parameters are optimized in ‘small-scale’ GSM+DMRG calculations, the final calculations can be performed in the large model space to obtain fully converged results.

In summary, this study describes the first application of the DMRG method to unbound many-fermion systems described by a complex-symmetric eigenvalue problem. The encouraging features of the proposed GSM+DMRG approach open the scope to systematic and high-precision studies of the continuum coupling effects in multiparticle OQS such as open microwave resonators, multi-electron open quantum dots, atomic nuclei, and atomic clusters close to the particle drip line.

This work was supported by the U.S. Department of Energy under Contracts Nos. DE-FG02-96ER40963 (University of Tennessee), DE-AC05-00OR22725 with UT-Battelle, LLC (Oak Ridge National Laboratory), and DE-FG05-87ER40361 (Joint Institute for Heavy Ion Research), and by the Spanish DGI under grant No. BFM2003-05316-c02-02.

- 
- [1] S.R. White, Phys. Rev. Lett. **69**, 2863 (1992); Phys. Rev. B **48**, 10345 (1993).
  - [2] J. Dukelsky and S. Pittel, Rep. Prog. Phys. **67**, 513 (2004).
  - [3] U. Schollwöck, Rev. Mod. Phys. **77**, 259 (2005).
  - [4] S.R. White and R. L. Martin, J. Chem Phys. **110**, 4127 (1999).
  - [5] J. Dukelsky and G. Sierra, Phys. Rev. Lett. **83**, 172 (1999).
  - [6] N. Shibata and D. Yoshioka, Phys. Rev. Lett. **86**, 5755 (2001).
  - [7] J. Dukelsky, S. Pittel, S.S. Dimitrova, and M. V. Stoitsov, Phys. Rev. C **65**, 054319 (2002).
  - [8] T. Papenbrock and D.J. Dean, J. Phys. G **31**, S1377 (2005).
  - [9] N. Michel, W. Nazarewicz, M. Płoszajczak, and J. Rotureau, Rev. Mex. Fisica **50**, 74 (2004).
  - [10] S. Pittel and N. Sandulescu, Phys. Rev. C **73**, 014301 (2006).
  - [11] I. McCulloch and M. Gulacsi, Europhys. Lett. **57**, 852 (2002).
  - [12] E. Carlon, M. Henkel, and U. Schollwöck, Eur. J. Phys. B **12**, 99 (1999).
  - [13] N. Michel, W. Nazarewicz, M. Płoszajczak and K. Benaceur, Phys. Rev. Lett. **89**, 042502 (2002); N. Michel, W. Nazarewicz, M. Płoszajczak, and J. Okołowicz, Phys. Rev. C **67**, 054311 (2003).
  - [14] R. Id Betan, R.J. Liotta, N. Sandulescu, and T. Vertse, Phys. Rev. Lett. **89**, 042501 (2002).
  - [15] T. Berggren, Nucl. Phys. A **109**, 265 (1968); T. Berggren and P. Lind, Phys. Rev. C **47**, 768 (1993).
  - [16] M. Barranco, J. Navarro, and A. Poves, Phys. Rev. Lett. **78**, 4729 (1997); R. Guardiola and J. Navarro, Phys. Rev. Lett. **84**, 1144 (2000).
  - [17] N. Michel, W. Nazarewicz, and M. Płoszajczak, Phys. Rev. C **70**, 064313 (2004).